NASA/TM-2005-213670

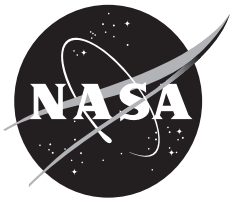

Local Flow Conditions for Proplusion Experiments on the F-15B Propulsion Flight Test Fixture

Michael J. Vachon, Timothy R. Moes, Stephen Corda
NASA Dryden Flight Research Center
Edwards, California

November 2005

NASA STI Program ... in Profile

Since its founding, NASA has been dedicated to the advancement of aeronautics and space science. The NASA scientific and technical information (STI) program plays a key part in helping NASA maintain this important role.

The NASA STI program is operated under the auspices of the Agency Chief Information Officer. It collects, organizes, provides for archiving, and disseminates NASA's STI. The NASA STI program provides access to the NASA Aeronautics and Space Database and its public interface, the NASA Technical Report Server, thus providing one of the largest collections of aeronautical and space science STI in the world. Results are published in both non-NASA channels and by NASA in the NASA STI Report Series, which includes the following report types:

- TECHNICAL PUBLICATION. Reports of completed research or a major significant phase of research that present the results of NASA programs and include extensive data or theoretical analysis. Includes compilations of significant scientific and technical data and information deemed to be of continuing reference value. NASA counterpart of peer-reviewed formal professional papers but has less stringent limitations on manuscript length and extent of graphic presentations.

- TECHNICAL MEMORANDUM. Scientific and technical findings that are preliminary or of specialized interest, e.g., quick release reports, working papers, and bibliographies that contain minimal annotation. Does not contain extensive analysis.

- CONTRACTOR REPORT. Scientific and technical findings by NASA-sponsored contractors and grantees.

- CONFERENCE PUBLICATION. Collected papers from scientific and technical conferences, symposia, seminars, or other meetings sponsored or co-sponsored by NASA.

- SPECIAL PUBLICATION. Scientific, technical, or historical information from NASA programs, projects, and missions, often concerned with subjects having substantial public interest.

- TECHNICAL TRANSLATION. English-language translations of foreign scientific and technical material pertinent to NASA's mission.

Specialized services also include creating custom thesauri, building customized databases, and organizing and publishing research results.

For more information about the NASA STI program, see the following:

- Access the NASA STI program home page at *http://www.sti.nasa.gov.*

- E-mail your question via the Internet to help@sti.nasa.gov.

- Fax your question to the NASA STI Help Desk at (301) 621-0134.

- Phone the NASA STI Help Desk at (301) 621-0390.

- Write to:
  NASA STI Help Desk
  NASA Center for AeroSpace Information
  7121 Standard Drive
  Hanover, MD 21076-1320

NASA/TM-2005-213670

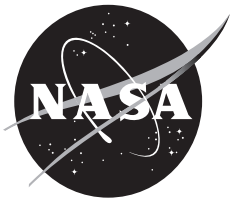

Local Flow Conditions for Proplusion Experiments on the F-15B Propulsion Flight Test Fixture

Michael J. Vachon, Timothy R. Moes, Stephen Corda
NASA Dryden Flight Research Center
Edwards, California

National Aeronautics and
Space Administration

Dryden Flight Research Center
Edwards, California 93523-0273

November 2005

NOTICE

Use of trade names or names of manufacturers in this document does not constitute an official endorsement of such products or manufacturers, either expressed or implied, by the National Aeronautics and Space Administration.

Available from the following:

NASA Center for AeroSpace Information
7121 Standard Drive
Hanover, MD 21076-1320
(301) 621-0390

National Technical Information Service
5285 Port Royal Road
Springfield, VA 22161-2171
(703) 605-6000

ABSTRACT

Local flow conditions were measured underneath the National Aeronautics and Space Administration F-15B airplane to support development of future experiments on the Propulsion Flight Test Fixture (PFTF). The local Mach number and flow angles were measured using a conventional air data boom on a cone-cylinder mounted under the PFTF and compared with the airplane air data nose boom measurements. At subsonic flight speeds, the airplane and PFTF Mach numbers were approximately equal. Transonic Mach number values were up to 0.1 greater at the PFTF than the airplane, which is a counterintuitive result. The PFTF local supersonic Mach numbers were as much as 0.46 less than the airplane values. The maximum local Mach number at the PFTF was approximately 1.6 at an airplane Mach number near 2.0. The PFTF local angle of attack was negative at all Mach numbers, ranging from –3 to –8 degrees. When the airplane angle of sideslip was zero, the PFTF local value was zero between Mach 0.8 and Mach 1.1, –2 degrees between Mach 1.1 and Mach 1.5, and increased from zero to 1 degree from Mach 1.5 to Mach 2.0. Airplane inlet shock waves crossed the aerodynamic interface plane between Mach 1.85 and Mach 1.90.

NOMENCLATURE

a_x	longitudinal acceleration, ft/s^2
a_z	vertical acceleration, ft/s^2
AFTF	Aerodynamic Flight Test Fixture
D	drag, lbf
g	acceleration due to gravity, ft/s^2
h	pressure altitude, ft
M_i	indicated Mach number obtained from the airplane air data nose boom
$M_{i,PFTF}$	PFTF local Mach number calculated using the cone-cylinder air data boom
M_{PC}	indicated Mach number corrected for static pressure position error
M_{PFTF}	local PFTF Mach number calculated using the airplane air data nose boom
NACA	National Advisory Committee for Aeronautics
NASA	National Aeronautics and Space Administration
P_S	specific excess power, ft/s
$p_{i,nb}$	airplane air data nose boom static pressure, uncorrected for static pressure position error, lbf/ft^2
pT	total pressure, lbf/ft^2
PFTF	Propulsion Flight Test Fixture
t	time, sec

T	thrust, lbf or temperature, °R
V	velocity, ft/s
W	weight, lbf
ΔM_{PC}	Mach number static pressure position error

INTRODUCTION

The NASA F-15B research test bed airplane has a unique capability to flight test propulsion devices, utilizing a Propulsion Flight Test Fixture (PFTF) that is hung underneath the airplane centerline (refs. 1 and 2). The PFTF provides a relatively inexpensive and efficient way to develop and flight test a wide range of propulsion devices and components. Propulsion hardware can be mounted to a six-component force balance underneath the fixture. The PFTF provides the support structure and volume for required propulsion systems, for example, propellant feed systems, control systems, and instrumentation. Subsonic, transonic, and supersonic flight data can be obtained up to airplane free-stream conditions of approximately Mach 2.0 and dynamic pressure of 1,100 lbf/ft^2 (52.67 kPa).

Knowledge of the local flow conditions upstream of the propulsive device is critical to the determination of performance and operability. The current flight tests obtained local flow conditions including Mach number, angle of attack, angle of sideslip, total pressure, static pressure, and shock wave location at the anticipated aerodynamic interface plane of a propulsive device mounted under the PFTF. Local conditions were compared to the airplane flow conditions.

AIRPLANE AND EXPERIMENT DESCRIPTIONS

The NASA F-15B is a platform uniquely qualified to support these flight tests. This high-performance research airplane is capable of accomplishing all desired test points while providing instrumentation recording, data telemetry, and real-time video. The PFTF utilized during this experiment was designed specifically for the NASA F-15B airplane. Flight test conditions and maneuvers were chosen based upon expected requirements for future experiments to be carried on the PFTF.

Airplane Description

The F-15B airplane is a two-seat trainer–fighter version of the F-15A high-performance, air-superiority fighter airplane built by McDonnell Aircraft Company (now The Boeing Company), St. Louis, Missouri. The F-15B airplane has a length of 63.7 ft (excluding the air data nose boom), a wingspan of 42.8 ft, and a height of 18.7 ft. The airplane is characterized by a shoulder-mounted main wing with a modified delta shape, twin vertical tails, all-moving horizontal stabilators, two engines mounted close together in the fuselage, and an elevated cockpit to enhance visibility. Primary flight control surfaces are controlled by a hydromechanical system and an electrical control augmentation system (CAS).

The F-15B airplane is powered by two Pratt & Whitney (West Palm Beach, Florida) F100-PW-100 turbofan engines that each produce an uninstalled, sea level static thrust of approximately 23,500 lbf in full afterburner. With these powerplants, the airplane is capable of dash speeds in excess of Mach 2.0 at altitudes of 40,000 to 60,000 ft. The airplane has a full-fuel takeoff weight of approximately 42,000 pounds and a landing weight of approximately 32,000 pounds. It has aerial refueling capability for extended-duration research missions.

The inlet system of the F-15B airplane consists of two two-dimensional, external compression, horizontal ramp inlets. Each inlet has three horizontal ramps mounted at the top of the inlet duct. The first ramp and upper cowl assembly rotate about a transverse hinge point at the lower cowl lip. Separate cowl and diffuser ramp actuators provide independent control of the first and third ramps, respectively. The second ramp position is dependent upon the first and third ramp positions. The second and third ramps, along with the side plates, are designed with porous bleed holes to remove the lower energy boundary layer flow. A fixed bypass bleed exit and a variable bypass door are provided for engine–inlet performance matching. At supersonic speeds, the bypass door is modulated to maintain the proper inlet throat Mach number. The system provides for a variable capture area that optimizes inlet performance, minimizes spillage drag, and maximizes inlet stability. The inlet system can be controlled automatically by the air inlet controller or, in an emergency, manually by the pilot.

The NASA F-15B airplane has been converted from an air-superiority fighter to a supersonic research test bed. Airplane modifications include the installation of research systems for the purposes of instrumentation, digital recording, telemetry, in-flight video, and global positioning system (GPS) navigation. A significant feature of the research capability of this airplane is the ability of the airplane to carry large experiment test fixtures on the lower fuselage centerline pylon. The fixtures installations are similar to the installation of a centerline fuel tank.

Experiment Description

The PFTF is a third generation research fixture that builds upon heritage from the development of the first and second generation Aerodynamic Flight Test Fixtures (AFTF), flown on NASA F-104 and F-15B airplanes, respectively (refs. 3 and 4). The PFTF complements the current inventory of F-15B airplane experiment flight test fixtures, the AFTF and the Centerline Instrumented Pylon (CLIP). The CLIP is a new fixture designed to accommodate larger span models underneath the airplane.

The PFTF is designed to be a flying engine test stand from which propulsion data can be obtained in the real flight environment. Advanced and prototype engines and propulsion technology can be carried and flight tested on the PFTF. The PFTF structure contains volume for propulsion system components such as fuel tanks, fluid systems, instrumentation, controllers, and other articles. A unique capability of the PFTF is the integral, six-component force balance. The balance permits the in-flight measurement of aerodynamic and propulsive forces.

The current flight test configuration is similar to that previously flown for the PFTF Cone-Drag Experiment (ref. 2), in which a cylinder with a conical nose and blunt base was carried below the

PFTF. Figure 1 shows the NASA F-15B airplane with the PFTF local flow experiment, in flight. The cylinder, including the conical nose, was 68 in. long with a diameter of 10 in. The conical nose was 13.5 in. long with a semi-apex angle of 20 deg. The PFTF and cone-cylinder weighed 868.3 lbs. Figure 2 shows the PFTF and cone-cylinder arrangement.

An attempt was made to mount the cylinder such that the local angle of attack and angle of sideslip were zero at a flight condition of Mach 1.5. This Mach number was selected based on the design point of several prospective experiments of interest at the time. Zero local angle of sideslip was set with respect to the airplane centerline. Zero local angle of attack was estimated by using local flow angle data from NASA F-15B/AFTF flight test data (ref. 4). While the AFTF configuration was considerably different from the current PFTF configuration, the AFTF data provided the best possible estimate. Based on the AFTF data, the PFTF cylinder angle of incidence was set at 2.5 deg nose up, with respect to the airplane air data nose boom centerline.

Instrumentation

Standard NACA air data nose booms built by SpaceAge Control, Inc. (Palmdale, California) were mounted on the NASA F-15B airplane nose and on the front of the cone-cylinder. Each air data boom measured the local total pressure, static pressure, angle of attack, and angle of sideslip. The air data boom contained two sets of static pressure ports separated by 0.75 in. The aft set of static pressure ports on the cone-cylinder air data boom were aligned with the aerodynamic interface plane. The measurements from the two sets of static pressure ports were averaged to obtain Mach number and altitude. The cone-cylinder air data boom was mounted with the angle of sideslip vane on the top side of the boom, contrary to standard air data boom installations that place the angle of sideslip vane on the bottom of the boom.

Conventional flow angle vanes, for measurement of angle of attack and angle of sideslip, were mounted downstream of the static pressure ports. Note that flow angle at the aerodynamic interface plane could not be measured with this configuration. The angle of attack and the angle of sideslip vanes were located 14.25 in. and 18.25 in., respectively, aft of the aerodynamic interface plane.

Three axis forces and moments were measured on the cone-cylinder using the integral PFTF force balance. Total temperature was measured by probes mounted on both the airplane and on the aft right side of the PFTF. Accelerometers were mounted on the fore and aft end of the cylinder to measure the cone-cylinder lateral and vertical accelerations. Other airplane measurements included linear and angular accelerations. All data were digitally recorded onboard the airplane and telemetered to ground-based recorders and control room displays in real time. Two video cameras, one facing forward and once facing aft, were mounted on the lower left of the airplane fuselage, aimed at the PFTF, and monitored in the aft cockpit and in the control room.

Flight Test Conditions and Maneuvers

Data were collected continuously from takeoff to landing. Maximum-power level accelerations were performed at pressure altitudes of 30,000 ft and 40,000 ft. The level accelerations were started at approximately Mach 0.8 and terminated at the maximum Mach number corresponding to the

1,100-psf dynamic pressure limit of the PFTF. Figure 3 shows the flight test points within the NASA F 15B/PFTF flight envelope. Only one level acceleration to maximum Mach number could be completed per flight because of airplane fuel limitations.

After reaching the maximum Mach number, level decelerations were performed at each altitude. Steady heading sideslips were performed at discrete Mach numbers during the decelerations to collect local sideslip data.

Two data flights were flown; one level acceleration at an altitude of 40,000 ft and one at an altitude of 30,000 ft. The flight test conditions for the two flights are shown in table 1. The actual deviations in the pressure altitude during the level accelerations were +0/–500 ft for the 40,000-ft altitude maneuver and +40/–600 ft for the 30,000-ft altitude maneuver.

Table 1. The NASA F-15B Propulsion Flight Test Fixture local flow flight test conditions.

Flight number	Mach number, start – end of level acceleration	Pressure altitude, ft (m)	Maximum dynamic pressure, lbf/ft^2 (N/m^2)	Pressure, lbf/ft^2 (N/m^2)	Temperature, °R (°K)
261	0.8 – 1.975	40,000 (12,192)	1069.5 (51,208)	391.7 (18,755)	390.0 (216.7)
262	0.8 – 1.55	30,000 (9,144)	1056.9 (50,605)	628.4 (30,088)	411.7 (228.7)

RESULTS AND DISCUSSION

Results are presented and discussed for the local flow conditions; Mach number, angle of attack, and angle of sideslip. Force balance and specific excess power data are also presented and discussed. In general, the local flow conditions are plotted as compared with the free-stream Mach number (M_{PFTF}). The free-stream Mach number is defined as the Mach number in the same vertical plane as the airplane air data nose boom but at the same altitude as the PFTF air data boom (see figure 2). Detailed tabular local flow data are contained in appendix A. This data may by used to aid in the planning of prospective propulsion experiments on the NASA F-15B/PFTF.

Local Mach Number

The local and free-stream Mach numbers are calculated from the total and static pressure measured by the cone-cylinder air data boom and airplane air data nose boom, respectively. The details of the Mach number calculation are given in appendix B.

Free-stream Mach number time histories for the 40,000-ft altitude and 30,000-ft altitude level acceleration or deceleration are shown in figures 4(a) and 4(b), respectively. The 40,000-ft altitude level acceleration was started at approximately Mach 0.84 and reached a maximum Mach number of 1.98. The 30,000-ft altitude level acceleration was started at approximately Mach 0.8 and reached a maximum of Mach 1.58. The acceleration of the airplane decreased with increasing Mach number, indicated by the continuous decrease in the slope of the lines in figures 4(a) and 4(b). Note that the acceleration remains positive at the end of the maneuver.

The PFTF local Mach number is compared with the free-stream Mach number in figures 5(a) and 5(b) for the 40,000-ft altitude and 30,000-ft altitude level acceleration or deceleration. A diagonal, dashed straight line drawn in each plot connects the points at which the free-stream and PFTF local Mach numbers are equal. As expected, the plots are similar for the two altitudes since the Reynolds numbers are similar. For the 30,000-ft altitude data, the Reynolds number range is from 2.278×10^6/ft to 4.414×10^6/ft. For the 40,000-ft altitude data, the Reynolds number range is from 1.526×10^6/ft to 3.768×10^6/ft.

Differences are seen between the acceleration and deceleration data, especially at transonic Mach numbers (approximately Mach 0.95 to Mach 1.2) and at Mach numbers between approximately Mach 1.47 and Mach 1.7 (at an altitude of 40,000 ft only). This may be due to hysteresis in the shock wave development or movement in shock location due to inlet spillage during deceleration. The largest differences occur at transonic speeds and at high Mach numbers when the F-15B airplane inlet shocks are approaching and then impinging upon the PFTF air data boom.

Figures 6(a) and 6(b) show the difference between the PFTF local Mach number and the free-stream Mach number. In general, the PFTF local Mach number is lower than the free-stream Mach number except in the transonic region between approximately Mach 0.995 and Mach 1.15. At subsonic speeds, the difference between the PFTF local and airplane Mach numbers is small.

For the level acceleration at an altitude of 40,000 ft, figure 6(a), the difference between the PFTF local Mach number and the airplane Mach number is increasingly negative. Subsonically, this reduction in Mach number ranged from approximately –0.02 at Mach 0.84 to a maximum of approximately –0.05 near Mach 1.0. The difference transitions dramatically very near Mach 1.0 such that the PFTF local Mach number is greater than the free-stream value until approximately Mach 1.15. Between free-stream Mach numbers of 1.15 and 1.86, the difference between PFTF local Mach number and the free-stream value becomes increasingly negative, differing from 0 to approximately –0.45. Beginning at Mach 1.86, the PFTF local Mach number increases discontinuously from approximately Mach 1.4 to Mach 1.55. This increase is likely caused by the passage of the F-15B airplane inlet shock across the cone-cylinder air data boom static pressure ports. The maximum free-stream Mach number of 1.978 corresponds to a PFTF local Mach number of 1.58.

The same trends in the Mach number differences are seen in the 30,000-ft altitude data, figure 6(b), although the absolute values are slightly different. The maximum Mach number achieved at an altitude of 30,000 ft was limited by the dynamic pressure limit imposed on the airplane to protect the PFTF force balance from potentially excessive side loads. The transition at which the

PFTF local Mach number is greater than the free-stream value is slightly longer at this altitude, lasting until a free-stream value of Mach 1.25. As tested at an altitude of 30,000 ft, the maximum free-stream Mach number of 1.55 corresponds to a PFTF local Mach number of 1.4.

Local Angle of Attack

The airplane air data nose boom and PFTF local angles of attack are plotted as a function of the airplane free-stream Mach number in figures 7(a) and 7(b) for the 40,000-ft altitude and 30,000-ft altitude test points. The PFTF local angle of attack is several degrees lower than the airplane angle of attack for all Mach numbers, indicating a local downwash flow field beneath the airplane. The PFTF local angle of attack is always negative for all Mach numbers, while the airplane angle of attack is always positive at all speeds at an altitude of 40,000 ft and up to Mach 1.35 at an altitude of 30,000 ft.

For the 40,000-ft altitude data, shown in figure 7(a), the PFTF local angle of attack has a roughly constant value of –2 to –4 deg between Mach 0.85 and Mach 1.3. At higher supersonic Mach numbers, the PFTF local angle of attack decreases almost linearly from approximately –2.5 deg at Mach 1.3 to –7.8 deg at Mach 1.98. Note that the airplane angle of attack decreases approximately linearly from Mach 0.85 to Mach 1.5, then remains constant at zero from Mach 1.5 to Mach 1.98.

The 30,000-ft altitude data, presented in figure 7(b), shows trends similar to the 40,000-ft altitude data of figure 7(a). The PFTF local angle of attack is fairly constant at –3 to –4 deg over the Mach number range from Mach 0.8 to approximately Mach 1.3. Above Mach 1.3, the PFTF local angle of attack shows a linear decrease. The airplane angle of attack shows a continual decrease throughout the Mach number range.

Local Angle of Sideslip

Angle of sideslip flight data are shown in figures 8(a) and 8(b) for an altitude of 40,000 ft, and in figures 9(a) and 9(b) for an altitude of 30,000 ft. The PFTF local angle of sideslip and the airplane air data nose boom angle of sideslip are shown plotted as compared with the free-stream Mach number. Figures 8(a) and 9(a) show airplane and local PFTF sideslip angles during constant-altitude accelerations for altitudes of 40,000 ft and 30,000 ft, respectively. No intentional sideslip was induced by pilot rudder input during these accelerations. Three steady heading sideslip maneuvers were performed as the airplane decelerated at constant altitude. These data are shown in figures 8(b) and 9(b) for the 40,000-ft altitude and 30,000-ft altitude level decelerations, respectively.

All of the PFTF local angle of sideslip data appear to be noisier than the airplane free-stream data. This noise may be caused by lateral vibration of the cone-cylinder assembly. However, the PFTF local angle of attack data did not show the same degree of unsteadiness.

During the level accelerations at both altitudes, the airplane angle of sideslip is benign, remaining within one degree of zero. Between approximately Mach 1.1 and Mach 1.5, the PFTF local angle of sideslip indicates approximately –2 deg (nose right) while the airplane measured angle of sideslip is near zero. Supersonically, from Mach 1.3 to Mach 2.0, the airplane angle of

sideslip is near zero. The PFTF local angle of sideslip changes dramatically from –2 deg to 0 deg at approximately Mach 1.5. Above approximately Mach 1.55, the local angle of sideslip increases from 0 to 1 deg (nose left).

During installation, the cone-cylinder air data boom was carefully aligned with the airplane air data nose boom for these tests, so it is not believed that the local sideslip was induced by misalignment of the cone-cylinder hardware. The phenomenon is believed to be a result of an airplane asymmetry and not a local fixture asymmetry because this mismatch in airplane and local angle of sideslip has been noted in subsequent flight tests with the AFTF mounted in place of the PFTF. Slight differences in the scheduling of the right and left F-15B airplane inlet ramps could cause this induced sideslip.

There are two principal differences between the PFTF and AFTF air data probe configurations. The PFTF air data boom is mounted at a 2.5-deg nose-up angle, and the angle of sideslip vane is situated on top of the boom. This positions the trailing edge of the vane within 10 in. of the leading edge of the PFTF pylon, and aerodynamic interaction with the detached pylon bow shock may be occurring at low supersonic speeds. For flight tests with the AFTF, the air data boom is always aligned with the F-15B airplane waterline and the angle of sideslip vane is mounted on the bottom of the boom, avoiding any potential aerodynamic influences.

Steady heading sideslips sweeps were performed at approximately Mach numbers 1.2, 1.4, and 1.8 during the 40,000-ft altitude level deceleration shown in figure 8(b) and at Mach numbers 1.1, 1.25, and 1.4 during the 30,000-ft altitude level deceleration shown in figure 9(b). Figures 8(b) and 9(b) compare the PFTF local flow sideslip angle obtained from the sideslip sweeps with the free-stream sideslip angle. The airplane sideslip input was a maximum of approximately 1.5 to 2 deg. The measured change in the local sideslip angle caused by the airplane sideslip input was approximately 0.5 to 1 deg less than input.

Note that at both altitudes, during the accelerations and decelerations, there is a repeatable double-spike in the PFTF local angle of sideslip just below an F-15B airplane free-stream Mach number of 1.1, but it is not reflected in the airplane sideslip data. The local angle of sideslip increases to as high as 2 deg and decreases to as low as –3 deg while the airplane sideslip remains constant. These spikes are believed to be a transonic phenomenon, possibly shock development or interaction with the sideslip vane; the airplane inlet asymmetry mentioned previously may be a contributing factor. These spikes in angle of sideslip have also been observed when flying the AFTF at similar Mach numbers.

Force Balance Data

PFTF force balance data was obtained for the cone-cylinder. The highest loads measured during the flight tests were with the airplane nose wheel landing gear extended. Previously collected vibration flight data have identified a low frequency vortex shedding from the nose wheel landing gear door that may be the cause of these higher loads (ref. 5). The force balance measured sinusoidal oscillations with a frequency of approximately 1 Hz during the level acceleration and deceleration maneuvers.

Specific Excess Power

Figures 10(a) and 10(b) show specific excess power (P_S) as a function of Mach number for the NASA F-15B airplane with the PFTF and cone-cylinder configuration for the 40,000-ft altitude and 30,000-ft altitude level accelerations. The specific excess power, shown in equation (1), was calculated using accelerometer data for the longitudinal acceleration (a_x) and the vertical acceleration (a_z).

$$P_S = \left(\frac{T - D}{W}\right)V = \frac{dh}{dt} + \frac{V}{g}\frac{dV}{dt} = a_z \Delta t + \frac{V}{g}a_x \qquad (1)$$

For both altitudes, the specific excess power remains positive at the completion of the level accelerations. The specific excess power increases subsonically to a maximum value, decreases transonically until past the transonic drag rise, then increases slightly until continually decreasing supersonically. At an altitude of 40,000 ft, the rise in P_S beginning at Mach 1.5 is a result of the higher efficiency obtained from the F-15B airplane variable geometry inlet as the inlet third ramp begins to schedule.

The specific excess power data shows that the F-15B airplane is aerodynamically capable of accelerating to higher Mach numbers, if needed, for future test points with the PFTF at an altitude of 40,000 ft, but has reached the limit of available power at an altitude of 30,000 ft.

CONCLUDING REMARKS

Flight tests were conducted to characterize the local flow underneath the NASA F-15B test bed research airplane in a region in which potential propulsion experiments could be carried. The Propulsion Flight Test Fixture (PFTF) with a cone-cylinder assembly was mounted underneath the F-15B airplane fuselage centerline. The cone-cylinder assembly is a dimensionally crude representation of a propulsion-type experiment. The local Mach number, angle of attack, and angle of sideslip data were compared between the airplane and the PFTF local flow. Maximum power, level accelerations were flown at pressure altitudes of 30,000 and 40,000 ft. Characteristics of the PFTF local flow are discussed below.

Local Mach Number

In subsonic flight, the PFTF local Mach number and airplane Mach number are approximately the same. In transonic flight, the PFTF local Mach number is approximately 0.1 greater than the airplane Mach number, which is a counterintuitive result. Above an airplane Mach number of 1.2, the difference between the airplane and PFTF local Mach numbers increases from 0.0 to 0.46 at an airplane Mach number of 1.86. The inlet shock wave crosses the PFTF cone-cylinder air data boom pressure ports at approximately Mach 1.86. At an airplane Mach number of 2.0, this shock passage results in a PFTF local Mach number of approximately 1.6. The F-15B airplane was

shown to have specific excess power at 40,000 ft for accelerating to higher Mach numbers.

Local Angle of Attack

The PFTF local angle of attack was negative at all Mach numbers, indicating a local downwash underneath the airplane. The PFTF local angle of attack was several degrees less than the airplane angle of attack at all Mach numbers, ranging from –3 to –8 deg.

Local Angle of Sideslip

The airplane angle of sideslip was essentially zero from subsonic Mach numbers to Mach 2.0. The PFTF local angle of sideslip averaged 0 deg from Mach 0.8 to Mach 1.1, approximately –2 deg (nose right) between Mach 1.1 and Mach 1.5, and up to +1 degree (nose left) above Mach 1.5.

These local flow measurements are for a specific configuration flown on the Propulsion Flight Test Fixture underneath the NASA F-15B airplane. They provide useful guidance in designing potential propulsion experiments for the NASA F-15B test bed airplane and valuable data for making preflight predictions.

Dryden Flight Research Center
National Aeronautics and Space Administration
Edwards, California, August 25, 2005

REFERENCES

1. Corda, Stephen, M. Jake Vachon, Nathan Palumbo, Corey Diebler, Ting Tseng, Anthony Ginn, and David Richwine, *The F-15B Propulsion Flight Test Fixture: A New Flight Facility for Propulsion Research*, NASA/TM-2001-210395, 2001.

2. Palumbo, Nathan, Timothy R. Moes, and M. Jake Vachon, *Initial Flight Tests of the F-15B Propulsion Flight Test Fixture*, NASA/TM-2002-210736, 2002.

3. Meyer, Robert R. Jr., *A Unique Flight Test Facility: Description and Results*, NASA TM-84900, 1982.

4. Richwine, David M., *F-15B/Flight Test Fixture II: A Test Bed for Flight Research*, NASA Technical Memorandum 4782, 1996.

5. Corda, Stephen, Russel J. Franz, James N. Blanton, M. Jake Vachon, and James B. DeBoer, *In-Flight Vibration Environment of the NASA F-15B Flight Test Fixture*, NASA/TM-2002-210719, 2002.

6. Ehernberger, L. J., Edward A. Haering, Jr., Mary G. Lockhart, and Edward H. Teets, "Atmospheric Analysis for Airdata Calibration on Research Aircraft," AIAA-92-0293, January 1992.

7. Shapiro, Ascher H., *The Dynamics and Thermodynamics of Compressible Fluid Flow, Volume 1,* The Ronald Press Company, New York, 1953.

APPENDIX A

LOCAL FLOW DATA

FLIGHT 261 ACCEL	Freestream Mach Number, M_{inf}	Time, t	Altitude, h	Dynamic Pressure, q	Longitudinal Acceleration, a_x	Vertical Acceleration, a_z	Freestream Total Pressure, $p_{T,inf}$	Freestream Static Pressure, $p_{s,inf}$	Local Total Pressure, $p_{T,local}$	Local Static Pressure, $p_{s,local}$	Freestream Angle of Attack, a_{nb}	Local Angle of Attack, a_{local}	Freestream Angle of Sideslip, b_{nb}	Local Angle of Sideslip, b_{local}
		sec	ft	lb/ft^2	g's	g's	lb/in^2	lb/in^2	lb/in^2	lb/in^2	deg	deg	deg	deg
	0.85	0.0	39996	198.3	0.154	0.956	4.37	2.78	4.52	2.89	3.99	-0.16	-0.43	-0.41
	0.90	19.4	40001	222.2	0.137	1.009	4.60	2.79	4.74	2.88	3.31	-0.45	-0.62	-0.44
	0.95	30.8	39995	247.1	0.279	0.956	4.86	2.81	5.02	2.91	2.48	-0.65	-0.74	0.12
	1.00	39.6	39957	275.0	0.210	0.934	5.16	2.86	5.33	2.64	2.64	-0.39	-0.62	0.48
	1.05	49.6	39941	303.4	0.228	0.934	5.48	2.73	5.66	2.74	2.62	-1.04	-0.68	-0.44
	1.10	58.4	39931	333.2	0.237	0.945	5.83	2.74	6.00	2.69	2.35	-0.65	-0.59	0.25
	1.15	67.8	39926	364.1	0.216	0.950	6.19	2.74	6.35	2.76	2.06	-0.39	-0.53	-0.90
	1.20	77.8	39918	396.5	0.206	0.998	6.58	2.74	6.75	2.84	1.93	-0.29	-0.19	-1.30
	1.25	87.6	39919	430.4	0.184	0.892	6.99	2.74	7.15	2.86	1.43	-0.97	-0.13	-1.63
	1.30	98.0	39918	465.4	0.172	0.977	7.41	2.74	7.67	2.94	1.29	0.16	-0.16	-1.89
	1.35	109.6	39911	501.9	0.148	0.945	7.86	2.74	8.13	3.05	1.04	-0.84	-0.03	-1.96
	1.40	125.2	39897	540.2	0.144	0.945	8.34	2.74	8.67	3.20	0.83	-1.23	0.00	-1.70
	1.45	137.8	39824	581.6	0.127	1.019	8.86	2.75	9.29	3.30	0.83	-1.85	0.55	-1.83
	1.50	156.0	39749	624.3	0.095	0.950	9.40	2.76	9.72	3.45	0.34	-2.04	0.00	-2.36
	1.55	172.2	39648	670.2	0.109	1.014	9.98	2.77	10.35	3.56	0.25	-2.46	0.00	0.75
	1.60	188.4	39532	717.8	0.118	0.966	10.58	2.78	11.11	3.68	0.14	-3.05	0.03	-0.01
	1.65	207.2	39515	764.0	0.114	0.987	11.17	2.78	11.54	3.84	0.08	-3.53	-0.10	0.75
	1.70	222.4	39577	808.7	0.088	0.902	11.73	2.77	12.48	4.02	-0.12	-3.83	-0.19	0.98
	1.75	243.0	39598	856.1	0.088	1.019	12.32	2.77	13.33	4.27	0.28	-3.73	-0.25	0.65
	1.80	268.6	39576	906.5	0.080	0.987	12.96	2.77	14.24	4.55	0.16	-4.28	-0.17	0.42
	1.85	295.6	39752	949.9	0.084	0.934	13.50	2.74	15.08	4.89	0.17	-4.57	-0.25	1.04
	1.90	321.2	39977	991.3	0.067	0.966	14.01	2.71	15.98	4.48	0.19	-4.77	-0.19	0.65
	1.95	354.8	40215	1032.4	0.053	0.934	14.51	2.68	16.98	4.62	0.22	-4.83	-0.11	1.11
	1.98	374.0	40334	1055.5	0.013	0.956	14.80	2.66	17.55	4.73	0.23	-5.25	-0.25	1.37

FLIGHT 261 DECEL	Freestream Mach Number, M_{inf}	Time, t	Altitude, h	Dynamic Pressure, q	Longitudinal Acceleration, a_x	Vertical Acceleration, a_z	Freestream Total Pressure, $p_{T,inf}$	Freestream Static Pressure, $p_{s,inf}$	Local Total Pressure, $p_{T,local}$	Local Static Pressure, $p_{s,local}$	Freestream Angle of Attack, a_{nb}	Local Angle of Attack, a_{local}	Freestream Angle of Sideslip, b_{nb}	Local Angle of Sideslip, b_{local}
		sec	ft	lb/ft^2	g's	g's	lb/in^2	lb/in^2	lb/in^2	lb/in^2	deg	deg	deg	deg
	1.98	0.0	40334	1055.5	0.013	0.956	14.80	2.66	17.55	4.73	0.23	-5.25	-0.25	1.37
	1.95	3.2	40356	1023.8	-0.520	1.019	14.39	2.66	17.52	4.64	0.22	-4.86	-0.08	1.54
	1.90	6.0	40378	972.3	-0.510	1.009	13.74	2.66	15.80	4.38	0.09	-4.86	0.18	0.61
	1.85	8.8	40407	920.5	-0.513	0.956	13.08	2.66	14.78	4.75	0.06	-4.47	-1.33	0.22
	1.80	11.8	40430	869.6	-0.476	1.083	12.43	2.66	13.74	4.41	0.34	-4.28	1.71	1.24
	1.75	14.8	40454	822.6	-0.460	0.902	11.84	2.66	12.93	4.16	-0.06	-3.99	0.89	1.11
	1.70	18.0	40475	775.6	-0.457	0.934	11.24	2.66	12.14	3.93	-0.09	-3.47	0.41	0.78
	1.65	21.4	40488	729.2	-0.431	0.956	10.66	2.66	11.40	3.70	-0.01	-3.57	0.13	0.12
	1.60	25.0	40505	684.8	-0.394	0.945	10.10	2.66	10.95	3.55	0.03	-2.82	-0.03	0.25
	1.55	28.8	40520	642.7	-0.360	0.987	9.57	2.66	10.35	3.49	0.14	-2.17	0.12	0.12
	1.50	33.0	40549	601.9	-0.328	0.998	9.06	2.66	9.69	3.38	0.28	-1.98	0.15	-2.06
	1.45	37.8	40562	561.0	-0.284	1.030	8.54	2.65	9.09	3.22	0.52	-1.43	0.82	-1.86
	1.40	42.8	40582	523.2	-0.256	0.987	8.07	2.65	8.51	3.08	0.58	-1.20	-0.33	-2.55
	1.35	48.6	40599	485.7	-0.220	0.924	7.61	2.65	8.01	2.97	0.65	-0.55	-0.13	-2.16
	1.30	55.2	40577	450.6	-0.217	1.019	7.18	2.65	7.49	2.89	1.17	0.00	0.06	-1.83
	1.25	61.8	40586	416.6	-0.212	0.934	6.76	2.65	7.05	2.79	1.21	-0.71	0.00	-2.19
	1.20	68.6	40585	384.3	-0.221	0.945	6.37	2.65	6.62	2.74	1.60	-1.20	-0.74	-1.89
	1.15	74.6	40567	352.2	-0.256	1.062	5.99	2.65	6.25	2.65	1.98	-0.26	-0.56	-1.56
	1.10	79.8	40580	322.9	-0.215	0.977	5.65	2.65	5.88	2.55	2.06	0.07	-0.46	-0.81
	1.05	86.0	40602	293.4	-0.204	0.924	5.30	2.65	5.52	2.47	2.09	-1.26	-0.22	-0.18
	1.00	91.4	40482	267.7	-0.177	1.099	5.03	2.79	5.26	2.52	2.39	-0.65	-0.33	-0.01
	0.95	100.4	40681	239.4	-0.071	1.025	4.71	2.72	4.94	2.83	2.21	-0.71	-0.39	-0.61
	0.90	113.2	40691	214.8	-0.043	0.913	4.45	2.70	4.65	2.79	2.52	-0.84	-0.10	-0.08
	0.85	127.8	40704	191.7	-0.007	0.977	4.22	2.68	4.44	2.79	3.50	-0.48	-0.03	-0.71

FLIGHT 262 ACCEL	Freestream Mach Number, M_{inf}	Time, t	Altitude, h	Dynamic Pressure, q	Longitudinal Acceleration, a_x	Vertical Acceleration, a_z	Freestream Total Pressure, $p_{T,inf}$	Freestream Static Pressure, $p_{s,inf}$	Local Total Pressure, $p_{T,local}$	Local Static Pressure, $p_{s,local}$	Freestream Angle of Attack, a_{nb}	Local Angle of Attack, a_{local}	Freestream Angle of Sideslip, b_{nb}	Local Angle of Sideslip, b_{local}
		sec	ft	lb/ft^2	g's	g's	lb/in^2	lb/in^2	lb/in^2	lb/in^2	deg	deg	deg	deg
	0.80	0.0	29956	282.5	0.178	0.902	6.67	4.45	6.84	4.55	2.47	-0.61	-0.37	-0.77
	0.85	8.2	29957	319.5	0.397	0.849	7.02	4.46	7.20	4.55	1.72	-0.87	1.35	0.78
	0.90	12.0	29946	357.0	0.475	1.019	7.40	4.49	7.53	4.55	1.72	-1.10	0.24	-0.15
	0.95	15.6	29994	398.2	0.443	0.913	7.81	4.51	7.96	4.58	1.15	-1.20	0.49	-0.15
	1.00	20.0	29958	441.0	0.341	1.051	8.28	4.59	8.39	4.15	1.69	-1.13	0.46	0.25
	1.05	25.8	29900	487.0	0.309	0.956	8.80	4.39	8.94	4.28	1.50	-0.94	0.55	0.35
	1.10	32.0	29882	535.5	0.263	0.971	9.36	4.40	9.51	4.20	1.29	-1.13	0.64	0.35
	1.15	39.4	29866	585.8	0.220	0.987	9.96	4.40	10.09	4.33	0.92	-0.81	0.70	-1.04
	1.20	48.6	29878	637.1	0.177	0.977	10.57	4.40	10.73	4.39	0.74	-1.07	0.79	-1.23
	1.25	60.2	29858	692.2	0.150	0.993	11.24	4.41	11.45	4.47	0.46	-0.65	1.16	-1.70
	1.30	74.4	29869	748.2	0.118	0.993	11.92	4.41	12.21	4.61	0.28	-0.65	1.07	-1.83
	1.35	91.4	29824	808.7	0.107	0.987	12.67	4.41	13.03	4.81	0.20	-0.87	0.73	-1.73
	1.40	110.2	29826	869.4	0.100	0.977	13.42	4.41	13.86	5.01	-0.06	-1.68	0.63	-1.80
	1.45	129.8	29815	932.8	0.078	0.871	14.21	4.41	14.79	5.24	-0.44	-2.11	0.06	-2.13
	1.50	158.6	29699	1003.5	0.045	0.945	15.10	4.43	15.90	5.50	-0.41	-2.37	0.17	-1.23
	1.55	199.8	29530	1080.1	0.042	1.083	16.08	4.46	17.01	5.66	-0.46	-2.72	0.53	0.65
	1.55	206.0	29555	1081.1	-0.187	0.966	16.09	4.46	17.06	5.67	-0.52	-2.66	0.49	0.55

FLIGHT 262 DECEL	Freestream Mach Number, M_{inf}	Time, t	Altitude, h	Dynamic Pressure, q	Longitudinal Acceleration, a_x	Vertical Acceleration, a_z	Freestream Total Pressure, $p_{T,inf}$	Freestream Static Pressure, $p_{s,inf}$	Local Total Pressure, $p_{T,local}$	Local Static Pressure, $p_{s,local}$	Freestream Angle of Attack, a_{nb}	Local Angle of Attack, a_{local}	Freestream Angle of Sideslip, b_{nb}	Local Angle of Sideslip, b_{local}
		sec	ft	lb/ft^2	g's	g's	lb/in^2	lb/in^2	lb/in^2	lb/in^2	deg	deg	deg	deg
	1.55	0.0	29499	1083.6	-0.218	0.998	16.13	4.47	17.16	5.69	-0.35	-2.95	0.43	0.35
	1.55	0.2	29497	1082.5	-0.198	0.902	16.11	4.47	17.18	5.72	-0.56	-2.88	0.27	0.05
	1.50	1.0	29492	1014.9	-0.528	0.966	15.27	4.48	16.16	5.63	-0.63	-2.59	0.33	-1.14
	1.45	4.2	29478	949.2	-0.482	0.945	14.45	4.48	15.11	5.35	-0.55	-2.62	1.38	-1.10
	1.40	2.0	29453	884.8	-0.426	0.908	13.65	4.49	14.28	5.14	-0.40	-1.49	-0.74	-2.29
	1.35	6.0	29410	822.9	-0.376	1.216	12.89	4.50	13.38	4.94	0.20	-1.07	0.82	-1.63
	1.30	3.0	29439	762.3	-0.334	0.902	12.14	4.49	12.52	4.71	0.06	-0.52	0.90	-1.73
	1.25	7.8	29480	704.5	-0.269	1.030	11.43	4.48	11.77	4.60	0.35	-0.42	-0.37	-1.83
	1.20	4.0	29523	647.3	-0.221	0.998	10.74	4.47	11.01	4.46	0.55	-0.84	0.13	-1.86
	1.15	1.0	29579	593.2	-0.160	0.940	10.08	4.46	10.32	4.36	0.74	-0.65	0.09	-0.84
	1.10	10.4	29695	539.6	-0.108	0.934	9.44	4.44	9.69	4.20	1.03	-0.84	-1.23	-1.00
	1.05	2.0	29837	488.5	-0.170	0.966	8.83	4.41	9.03	4.06	1.09	-0.81	0.21	0.45
	1.00	7.0	29740	446.5	-0.276	1.104	8.37	4.64	8.61	4.09	1.49	-1.39	0.61	-0.05
	0.95	3.0	29957	398.1	-0.075	1.014	7.82	4.52	8.04	4.65	1.23	-1.17	0.79	0.35
	0.90	18.2	29937	357.3	-0.073	0.987	7.40	4.49	7.62	4.52	1.27	-1.30	0.67	-0.11
	0.85	4.0	29922	318.9	-0.119	0.982	7.02	4.47	7.26	4.50	1.46	-0.91	0.98	0.09
	0.80	15.2	29940	282.4	-0.045	0.961	6.67	4.45	6.89	4.54	2.22	-0.81	0.30	0.25

APPENDIX B

MACH NUMBER CALCULATION

The airplane freestream Mach number corrected for static pressure position error, M_{PC}, is given by equation (B.1), where M_i is the indicated Mach number obtained from the airplane air data nose boom and ΔM_{PC} is the Mach number static pressure position error.

$$M_{PC} = M_i + \Delta M_{PC} \tag{B.1}$$

Note that the airplane nose boom indicated Mach number is not the cockpit indicated Mach number. The cockpit indicated Mach number is obtained from the production air data system of the F-15B airplane and incorporates a production static pressure position error correction.

Airplane Air Data Nose Boom Indicated Mach Number

The radar-rawinsonde method of reference 6 is used to calculate the indicated Mach number. The static pressure is assumed to be a function of geometric altitude and is obtained from rawinsonde data gathered on the day of the flight test. The F-15B airplane indicated Mach number is calculated from the airplane air data nose boom total and static pressures p_T and $p_{i,nb}$, respectively, using the appropriate relationships for subsonic and supersonic flow.

Subsonic flow, M < 1.0:

For subsonic flow, the Mach number is calculated from the isentropic relationship for the total-to-static pressure ratio shown in equation (B.2), where γ is the ratio of specific heats (for air, $\gamma = 1.4$).

$$\frac{p_T}{p_{i,nb}} = \left(1 + \frac{\gamma - 1}{2} M_{ind}^2\right)^{\frac{\gamma}{\gamma - 1}} \tag{B.2}$$

Equation (B.2) can be solved directly for the indicated Mach number as shown in equation (B.3).

$$M_{ind} = \left[\frac{2}{\gamma - 1}\left(\left(\frac{p_T}{p_{i,nb}}\right)^{\left(\frac{\gamma - 1}{\gamma}\right)} - 1\right)\right]^{0.5} \tag{B.3}$$

Supersonic flow, M > 1.0:

For supersonic flow, a normal shock wave is assumed to be positioned ahead of the mouth of the air data boom. Therefore, the Rayleigh pitot tube formula for inviscid, adiabatic, supersonic flow is utilized as shown in equation (B.4):

$$\frac{p_T}{p_s} = \frac{\left(1 + \frac{\gamma - 1}{2} M_{ind}^2\right)^{\frac{\gamma}{\gamma - 1}}}{\left(\frac{2\gamma}{\gamma + 1} M_{ind}^2 \frac{\gamma - 1}{\gamma + 1}\right)^{\frac{1}{\gamma - 1}}} \tag{B.4}$$

In equation (B.4), p_T is the total pressure downstream of the shock wave and p_s is the static pressure upstream of the shock wave. The air data boom measures total and static pressures downstream of the shock wave. Experimental data indicates that if the static pressure measurement tap on the air data probe is placed at least ten probe diameters downstream of the probe nose, the static pressure measurement is a close approximation to the static pressure upstream of the shock wave (ref. 7). Therefore, the static pressure, p_s, in equation (B.4) is equal to the air data probe static pressure, $p_{i,nb}$.

Since the Rayleigh pitot tube formula cannot be solved directly for Mach number, a polynomial curve fit to equation (B.4) is used to calculate Mach number as shown in equation (B.5).

$$M_{ind} = \left[\frac{\left(1.4285 - 0.357143x - 0.0625x^2 - 0.25x^3 - 0.012617x^4 - 0.00715x^5 - 0.004358x^6 - 0.0087725x^9\right)}{x}\right]^{0.5} \tag{B.5}$$

where

$$x = \frac{1.83937}{p_T / p_{i,nb}} \tag{B.6}$$

Figure B.1 shows a comparison of the curve fit [equation (B.5)] with Rayleigh pitot tube formula [equation (B.4)].

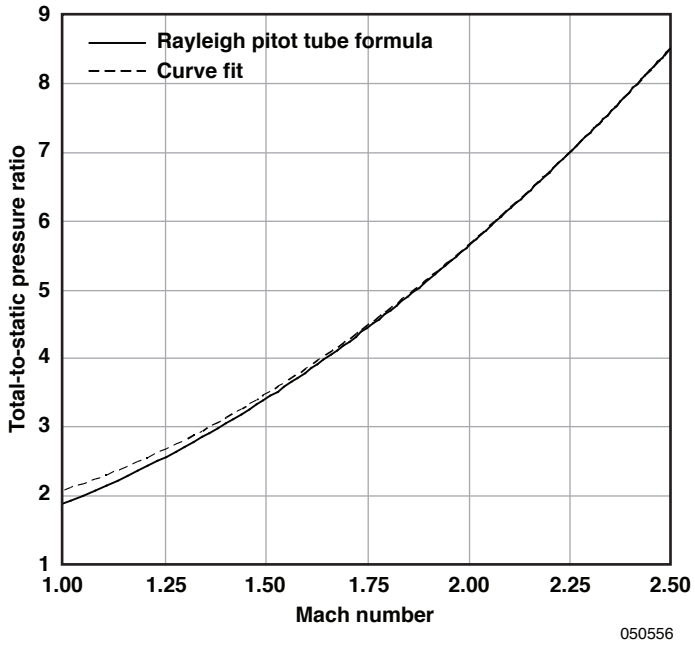

Mach Number Static Pressure Position Error

The F-15B airplane ΔM_{PC} has been obtained through flight comparison of the air data nose boom Mach number with a true Mach number that is independent of position error. The true Mach number is calculated from global positioning system (GPS) flight data combined with weather balloon data. The difference between the true and indicated Mach number is defined as ΔM_{PC}. F-15B airplane flight tests have been performed to determine this correction as a function of indicated Mach number, as shown in table B.1.

Table B.1. The F-15B airplane Mach number static pressure position error.

F-15B Indicated Mach number, M_i	Mach number static pressure position error, ΔM_{PC}
0.000	0.0000
0.300	0.0045
0.400	0.0068
0.500	0.0091
0.600	0.0116
0.700	0.0146
0.800	0.0188
0.850	0.0217
0.900	0.0260
0.930	0.0296
0.950	0.0360
0.965	0.0500
1.015	0.0020
1.200	0.0028
1.400	0.0032
1.600	0.0032
2.000	0.0000
2.100	0.0000

Free-stream Conditions

The M_{PC} is calculated using equation (B.1) as the sum of M_i, calculated from equation (B.2) or (B.3), and ΔM_{PC}, from table B.1. After M_{PC} has been calculated, a free-stream static pressure, P_∞, is calculated from equation (B.2) or (B.3), assuming the p_T has not changed, that is, that the total pressure position error is zero. Altitude and dynamic pressure are calculated from the free-stream static pressure.

FIGURES

EC04 0176-06

Figure 1. The NASA F-15B airplane with the Propulsion Flight Test Fixture local flow experiment, in flight.

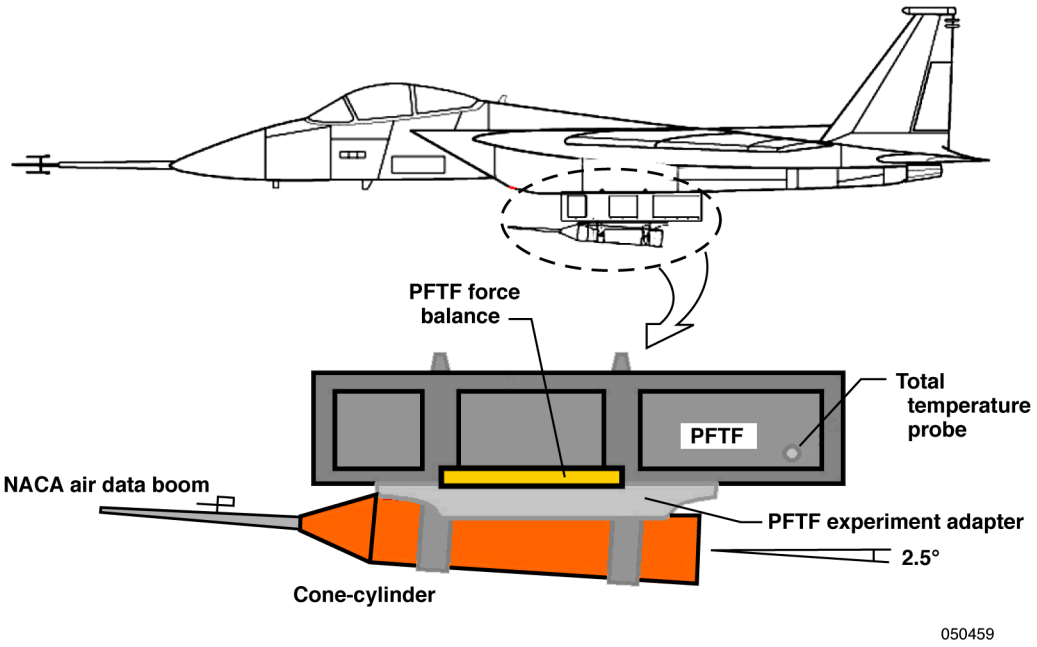

Figure 2. The Propulsion Flight Test Fixture and cone-cylinder arrangement on the NASA F-15B airplane.

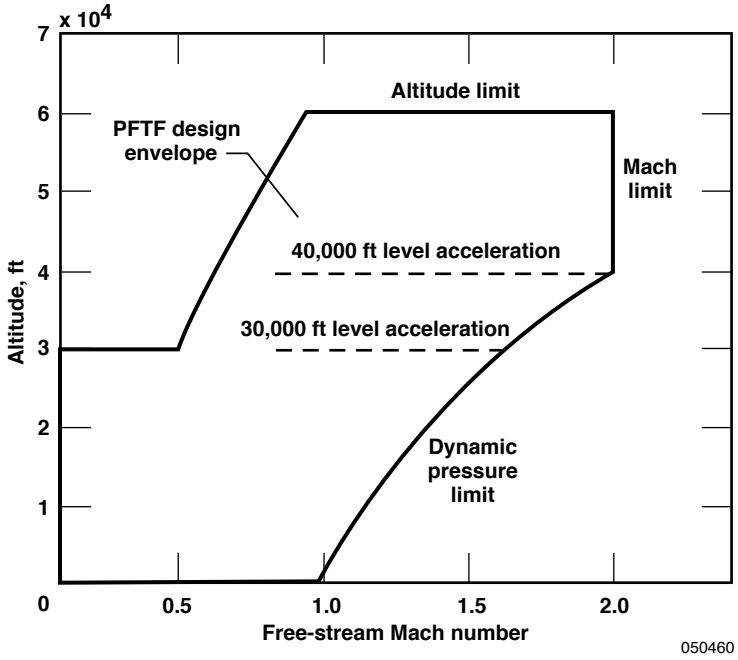

Figure 3. The NASA F-15B/PFTF flight envelope and flight test points.

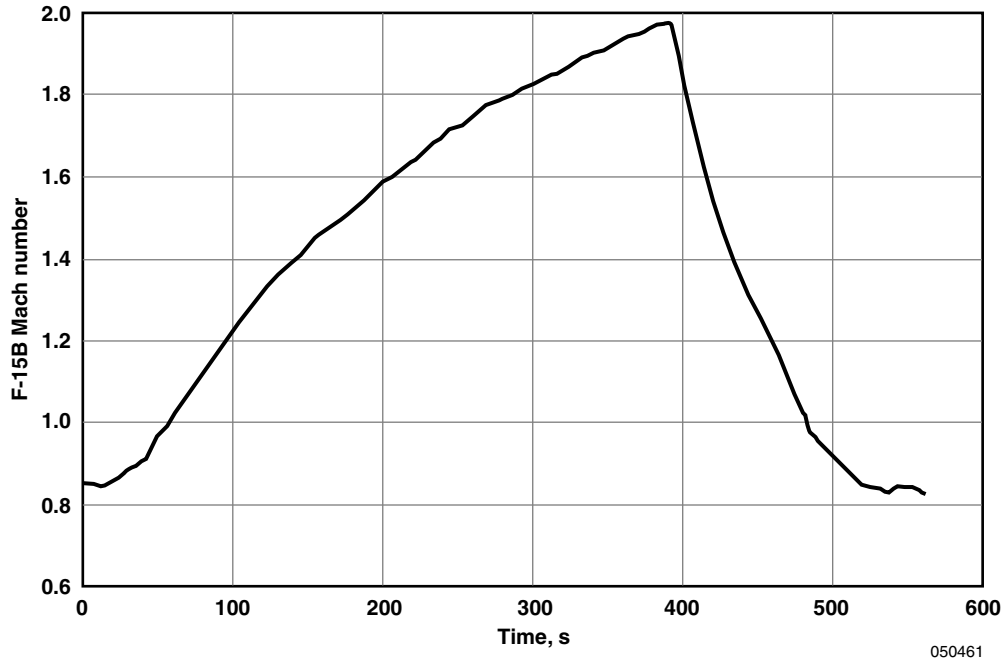

(a) Level acceleration and deceleration at an altitude of 40,000 feet.

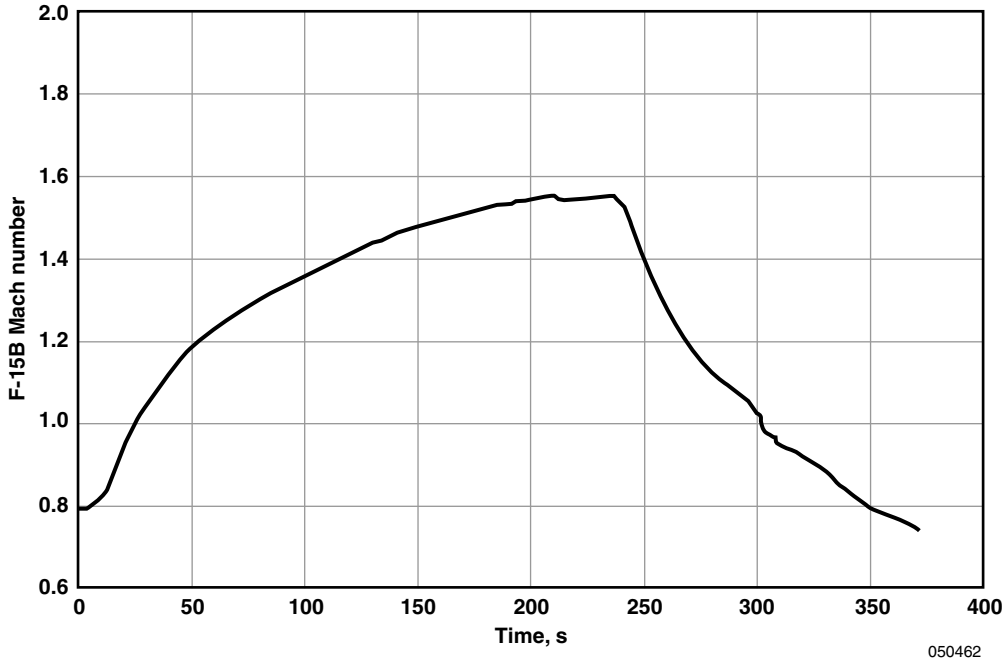

(b) Level acceleration and deceleration at an altitude of 30,000 feet.

Figure 4. The NASA F-15B airplane free-stream Mach number time histories.

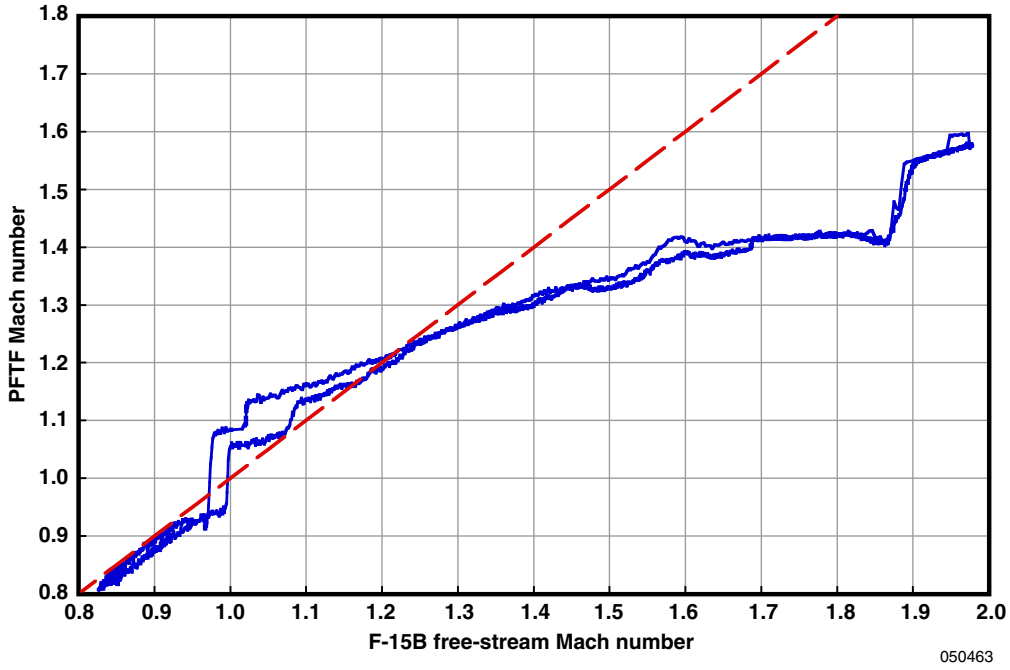

(a) Level acceleration and deceleration at an altitude of 40,000 feet.

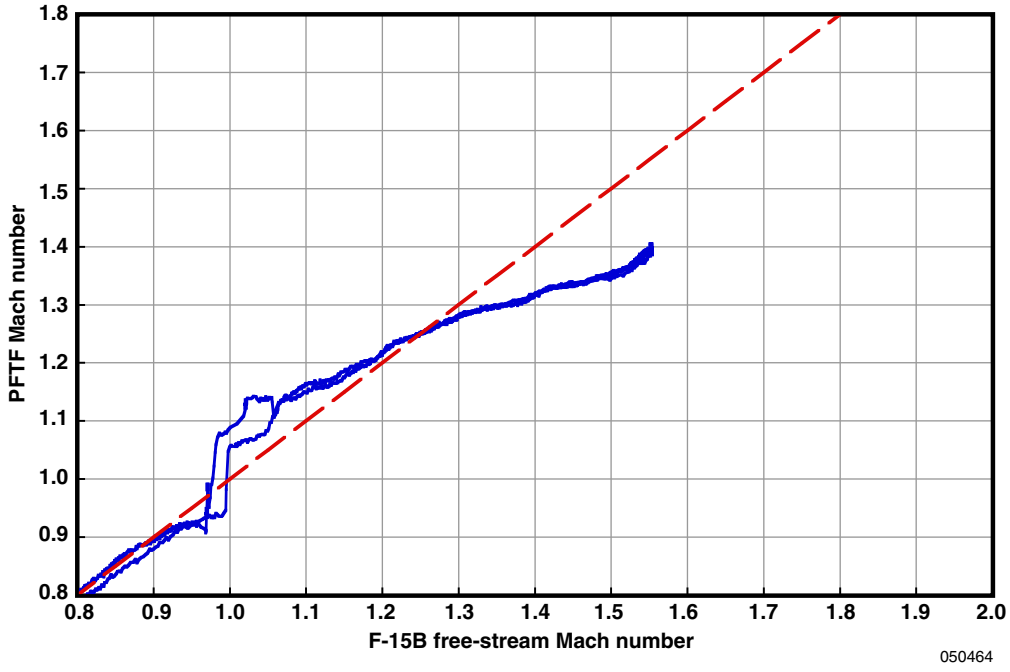

(b) Level acceleration and deceleration at an altitude of 30,000 feet.

Figure 5. The NASA F/15B/PFTF local Mach number as compared with free-stream Mach number.

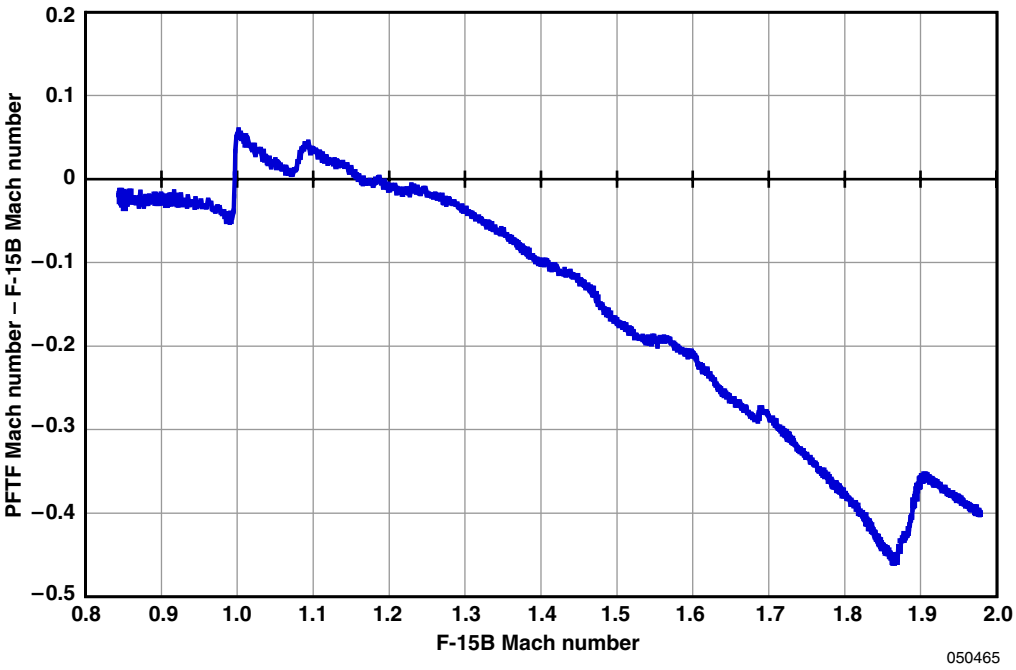

(a) Level acceleration at an altitude of 40,000 feet.

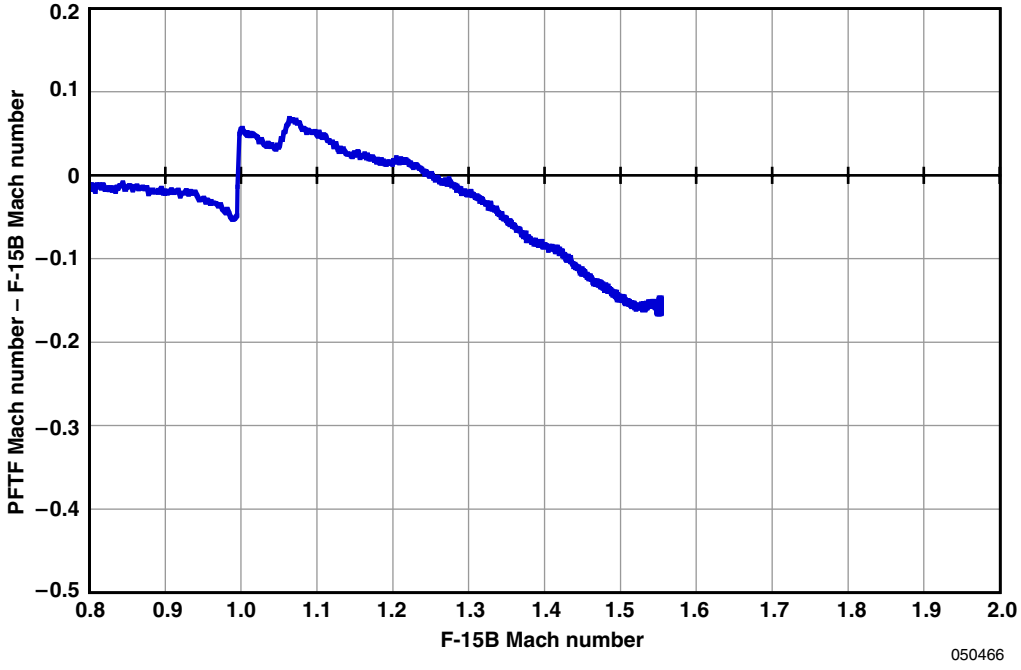

(b) Level acceleration at an altitude of 30,000 feet.

Figure 6. The difference between the NASA F-15B/PFTF local Mach number and the free-stream Mach number.

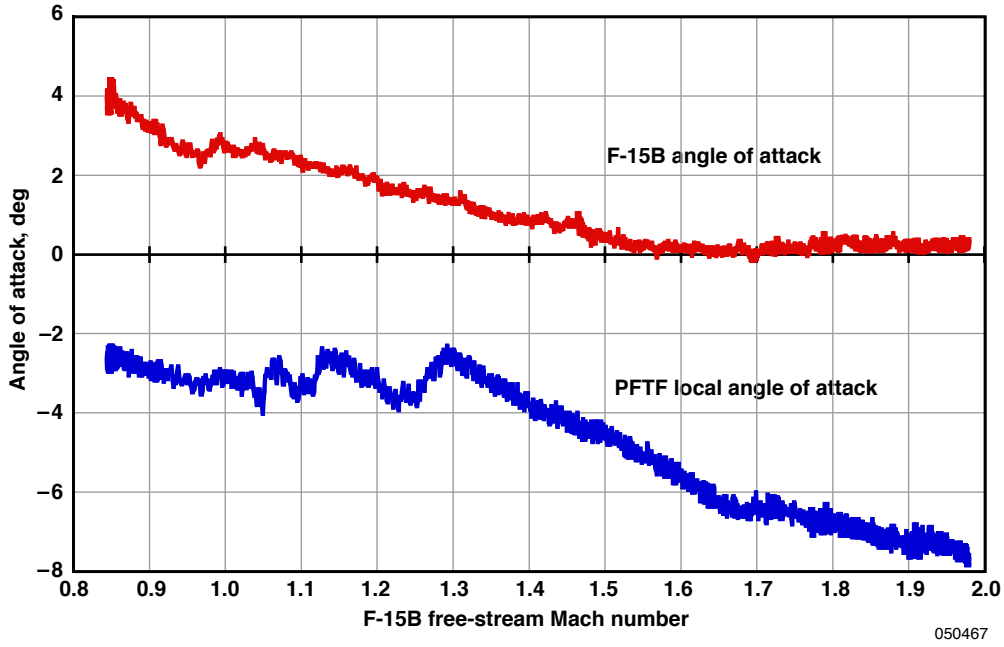

(a) Level acceleration at an altitude of 40,000 feet.

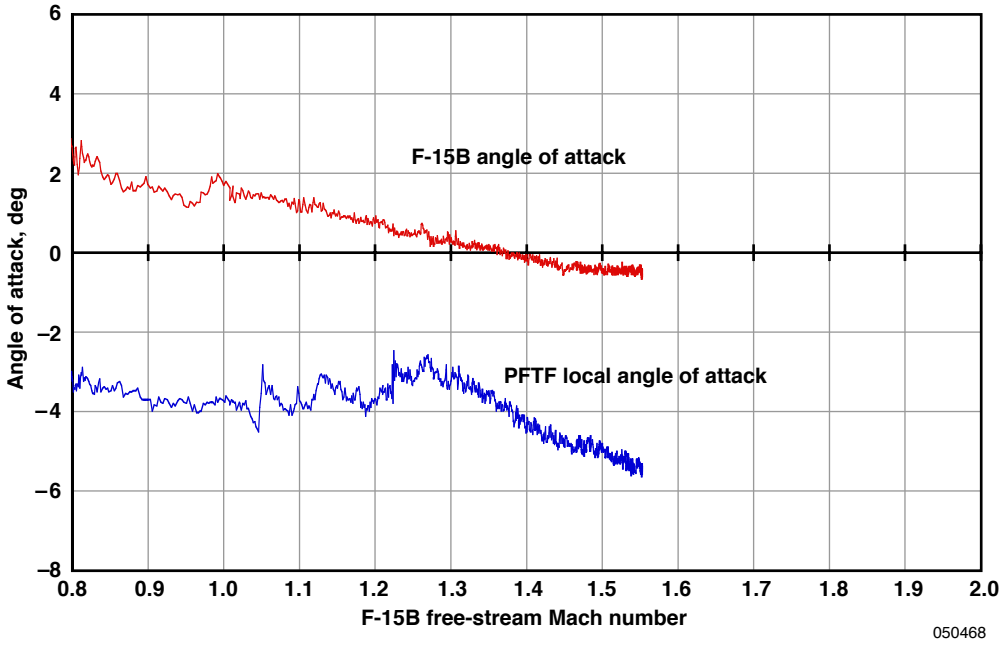

(b) Level acceleration at an altitude of 30,000 feet.

Figure 7. The local angle of attack as compared with the free-stream Mach number.

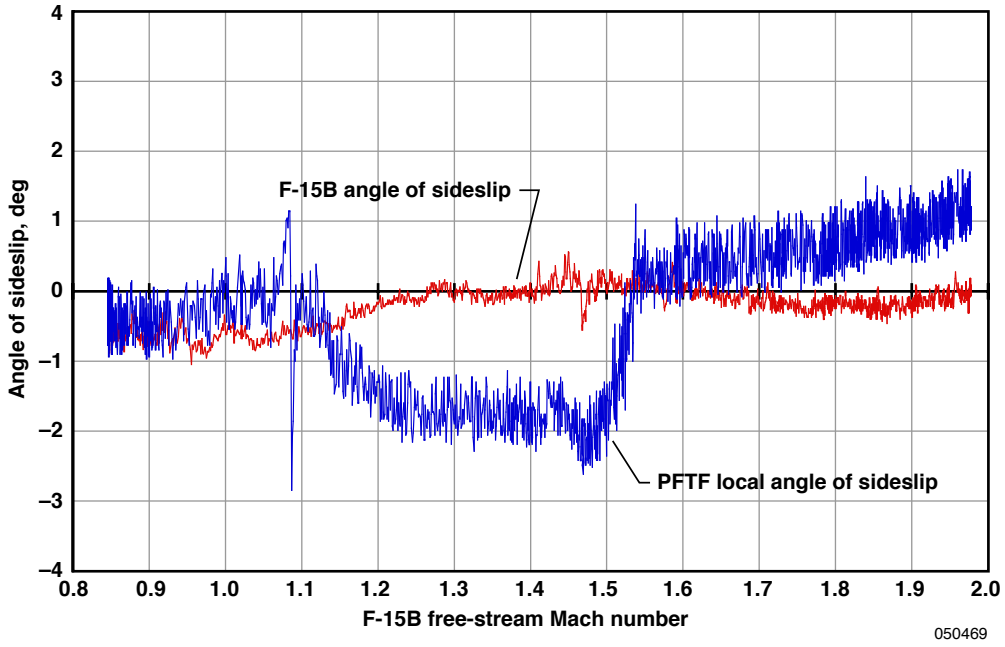

(a) Level acceleration.

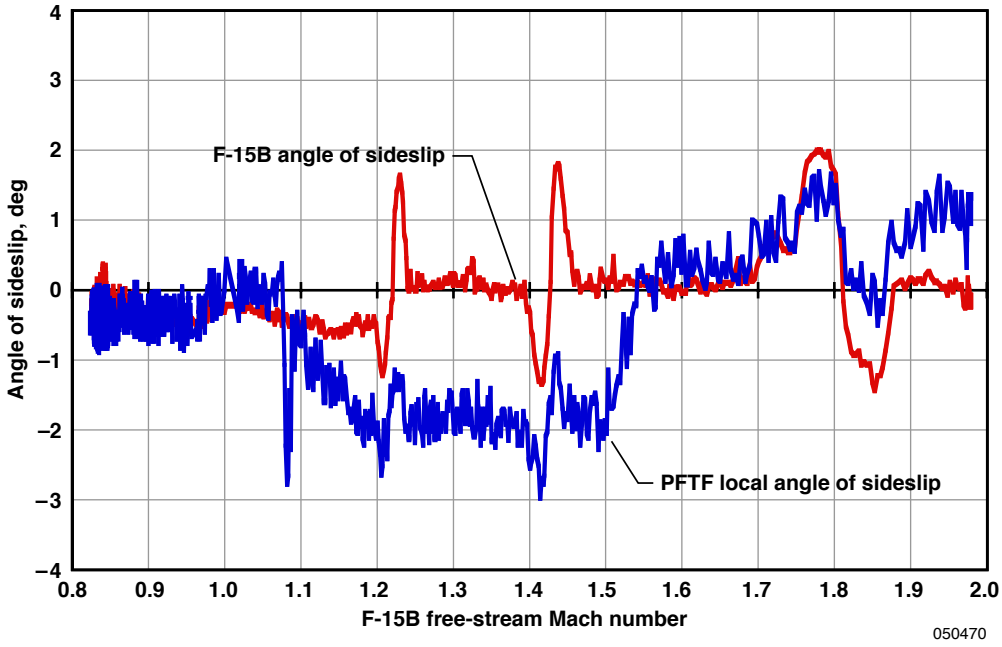

(b) Level deceleration.

Figure 8. The local angle of sideslip as compared with the free-stream Mach number at an altitude of 40,000 ft.

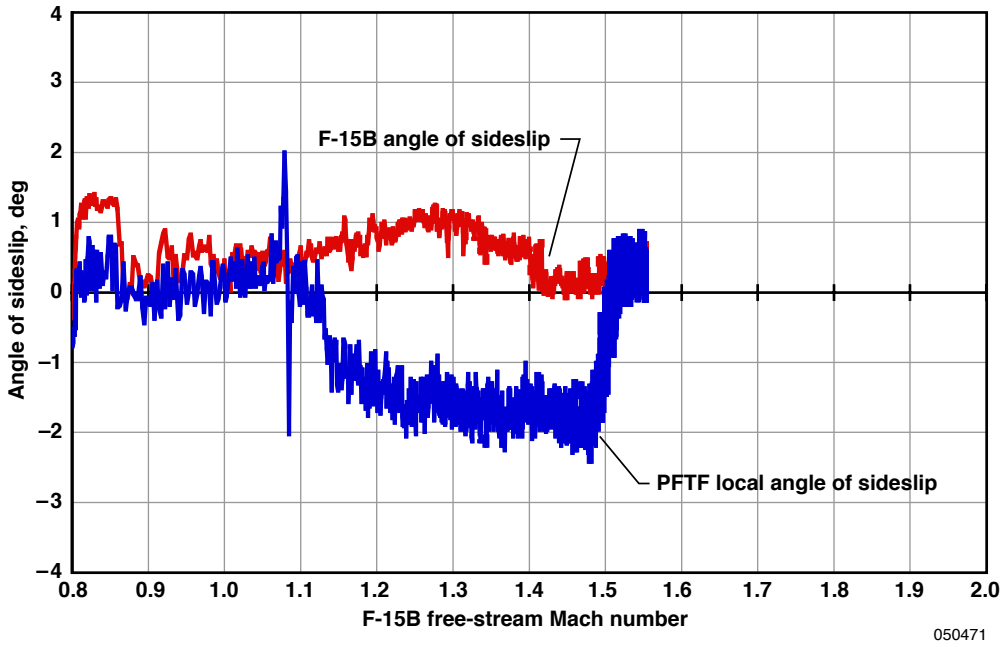

(a) Level acceleration.

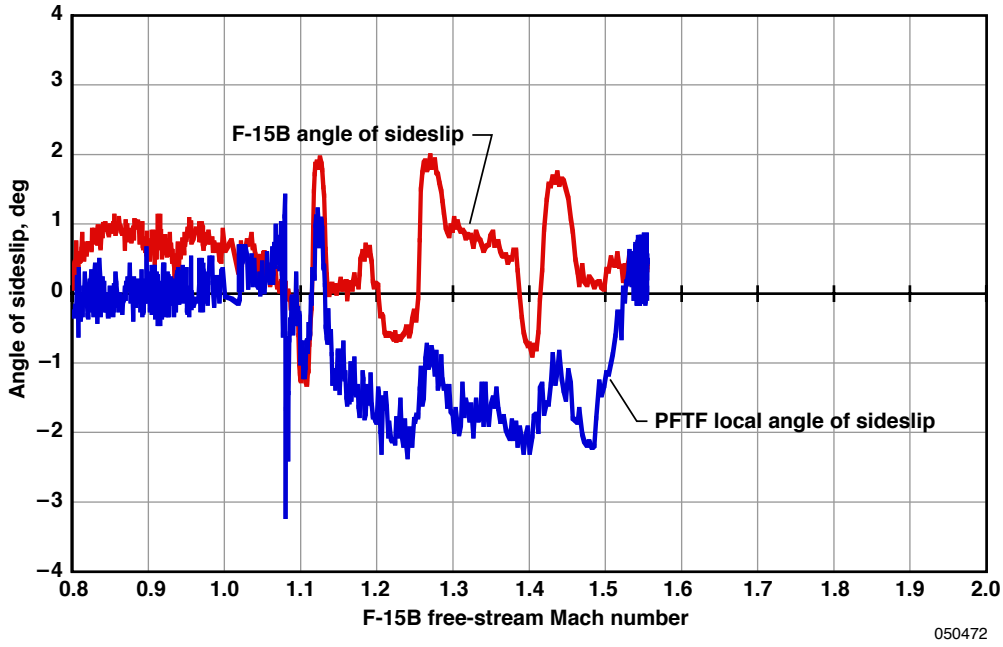

(b) Level deceleration.

Figure 9. The local angle of sideslip as compared with the free-stream Mach number at an altitude of 30,000 ft.

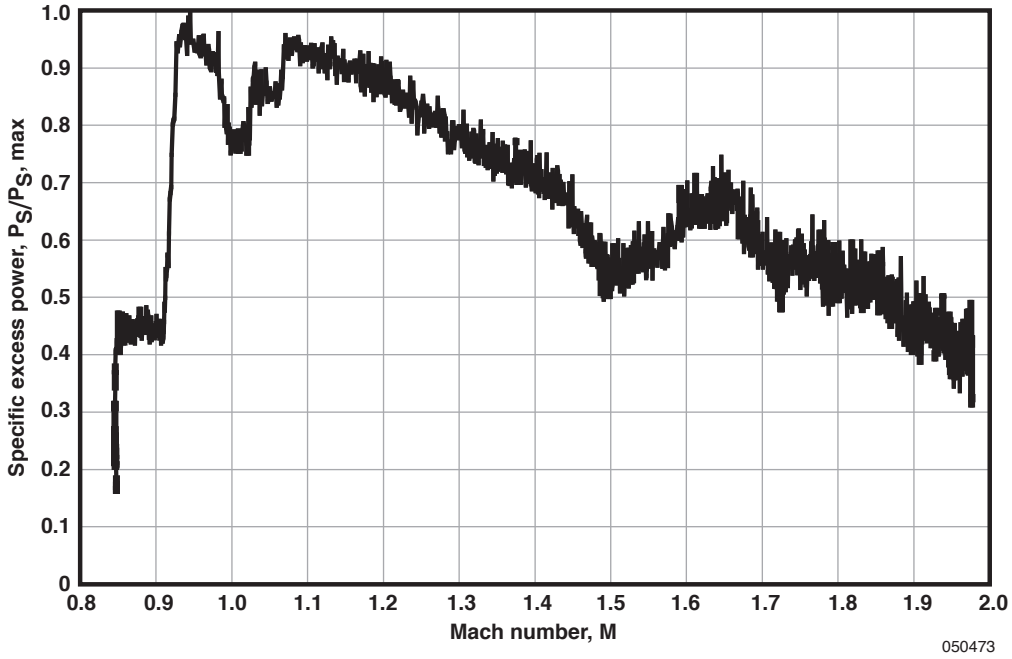

(a) Level acceleration at an altitude of 40,000 feet.

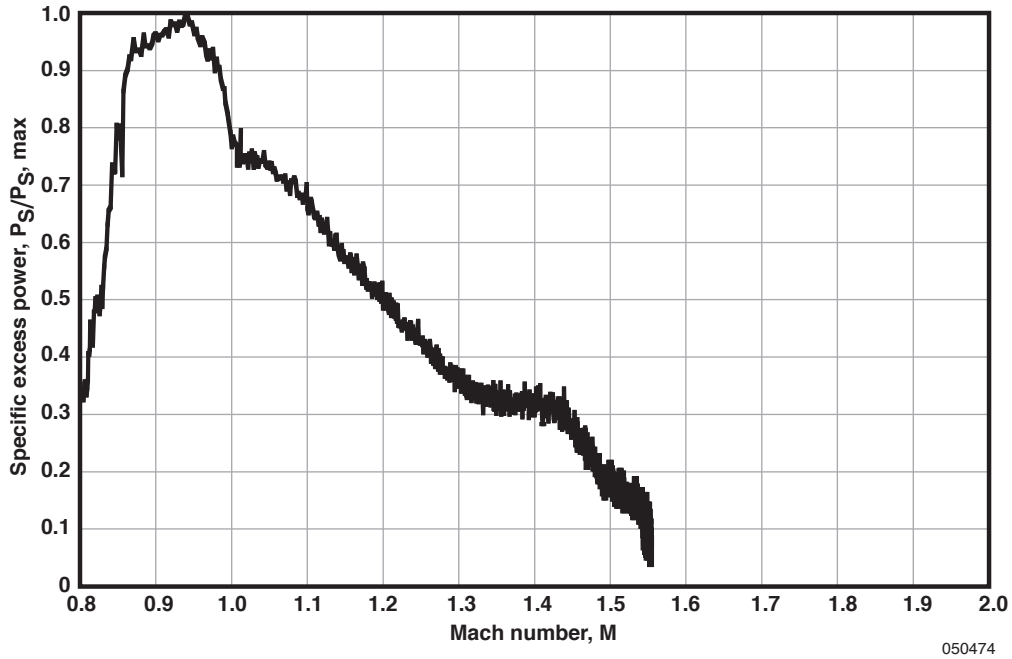

(b) Level acceleration at an altitude of 30,000 feet.

Figure 10. The NASA F-15B/PFTF local flow experiment specific excess power.

REPORT DOCUMENTATION PAGE

Form Approved
OMB No. 0704-0188

1. REPORT DATE *(DD-MM-YYYY)*	2. REPORT TYPE	3. DATES COVERED *(From - To)*
25-11-2005	Technical Memorandum	

4. TITLE AND SUBTITLE
Local Flow Conditions for Propulsion Experiments on the NASA F-15B Propulsion Flight Test Fixture

5a. CONTRACT NUMBER

5b. GRANT NUMBER

5c. PROGRAM ELEMENT NUMBER

6. AUTHOR(S)
Michael Jacob Vachon, Timothy R. Moes, and Stephen Corda

5d. PROJECT NUMBER

5e. TASK NUMBER

5f. WORK UNIT NUMBER
24-723-01-000-AAA

7. PERFORMING ORGANIZATION NAME(S) AND ADDRESS(ES)
NASA Dryden Flight Research Center
P.O. Box 273
Edwards, California 93523-0273

8. PERFORMING ORGANIZATION REPORT NUMBER
H-2625

9. SPONSORING/MONITORING AGENCY NAME(S) AND ADDRESS(ES)
National Aeronautics and Space Administration
Washington, DC 20546-001

10. SPONSORING/MONITOR'S ACRONYM(S)
NASA

11. SPONSORING/MONITORING REPORT NUMBER
NASA/TM-2005-213670

12. DISTRIBUTION/AVAILABILITY STATEMENT
Unclassified -- Unlimited
Subject Category -- 02, 05, 07 Availability: NASA CASI (310) 621-0390 Distribution: Standard

13. SUPPLEMENTARY NOTES
An electronic version can be found at the NASA Dryden Flight Research Center Web site, under Technical Reports.

14. ABSTRACT

Local flow conditions were measured underneath the National Aeronautics and Space Administration F-15B airplane to support development of future experiments on the Propulsion Flight Test Fixture (PFTF). The local Mach number and flow angles were measured using a conventional air data boom on a cone-cylinder mounted under the PFTF and compared with the airplane air data nose boom measurements. At subsonic flight speeds, the airplane and PFTF Mach numbers were approximately equal. Transonic Mach number values were up to 0.1 greater at the PFTF than the airplane, which is a counterintuitive result. The PFTF local supersonic Mach numbers were as much as 0.46 less than the airplane values. The maximum local Mach number at the PFTF was approximately 1.6 at an airplane Mach number near 2.0. The PFTF local angle of attack was negative at all Mach numbers, ranging from -3 to -8 degrees. When the airplane angle of sideslip was zero, the PFTF local value was zero between Mach 0.8 and Mach 1.1, -2 degrees between Mach 1.1 and Mach 1.5, and increased from zero to 1 degree from Mach 1.5 to Mach 2.0. Airplane inlet shock waves crossed the aerodynamic interface plane between Mach 1.85 and Mach 1.90.

15. SUBJECT TERMS
Advanced propulsion systems, Air breathing engines, F-15 aircraft, Flight test fixture, Flight tests, Flow characteristics, Inlet flow, Inlet nozzles, Nozzle flow, Rocket-based combined-cycle engines, Testbed

16. SECURITY CLASSIFICATION OF:			17. LIMITATION OF ABSTRACT	18. NUMBER OF PAGES	19a. NAME OF RESPONSIBLE PERSON
a. REPORT	b. ABSTRACT	c. THIS PAGE			STI Help Desk (email: help@sti.nasa.gov)
					19b. TELEPHONE NUMBER *(Include area code)*
U	U	U	U	33	(310) 621-0390